sition in the computations to better simulate the real physics of the flow at low M_∞ and high α does not degrade the computations at high M_∞ and low α, where the onset of unsteady flow is still caused by turbulent shock induced boundary-layer separation. These results with simple point transition suggest a pressing need for a turbulence model that provides for the natural transition from laminar to turbulent flow, particularly when attempting to compute unsteady flows at low Mach numbers and high angles of attack.

Experimental and computed buffet boundaries for the supercritical airfoil section are compared in Fig. 3. Agreement with experiment is very good at $M_\infty > 0.7$; however, at lower M_∞ and higher α the computed buffet boundary occurs at values of C_ℓ that are 10% higher than experiment. Also shown at $M_\infty = 0.6$ is the C_ℓ computed for the onset of unsteady flow with point transition fixed at $x/c = 0.24$. This result further demonstrates the need for a turbulence model that accounts for natural transition from laminar to turbulent flow. Compared with the similar reduction in mean lift coefficient for the conventional airfoil (see Fig. 1), the supercritical airfoil indicates at least an equal sensitivity to the numerical simulation of an upper surface leading-edge separation bubble. Whether such a sensitivity exists in actual experiments remains to be determined.

Concluding Remarks

An implicit finite difference computer code for solving the thin-layer compressible Navier-Stokes equations has been programmed for the ILLIAC IV computer and used to compute the buffet boundaries of a conventional and a supercritical airfoil section at high Reynolds numbers. Agreement between the computed and available experimentally determined buffet boundaries is very good at the higher freestream Mach numbers and lower lift coefficients where the onset of unsteady flows is associated with shock-wave induced boundary-layer separation. At the lower Mach numbers and higher angles of attack where the onset of unsteady flows is associated with an upper surface leading-edge separation bubble (and a weak shock wave as well) the computed boundaries are not in good agreement with experiment but can be improved by accounting, even in a crude way, for boundary-layer transition. The results indicate a pressing need for turbulence models that can simulate the natural transition from laminar to turbulent flow.

References

[1] Gadberg, B. L. and Ziff, H. L., "Flight Determined Buffet Boundaries of Ten Airplanes and Comparisons with Five Buffeting Criteria," NACA RM A50I27, Jan. 1951.

[2] Polentz, P. P., Page, W. A., and Levy, L. L. Jr., "Unsteady Normal-Force Characteristic of Selected NACA Profiles at High Subsonic Mach Numbers," NACA RM A55C02, May 1955.

[3] Ohman, L. H., Kacprzynski, J. J., and Brown, D., "Some Results from Tests in the NAE High Reynolds Number Two-Dimensional Test Facility on Shockless and Other Airfoils," *Canadian Aeronautics and Space Journal*, Vol. 19, 1973, pp. 297-312.

[4] Roos, F. W. and Riddle, D. W., "Measurements of Surface-Pressure and Wake Flow Fluctuations in the Flow Field of a Whitcomb Supercritical Airfoil," NASA TN D-8443, Aug. 1977.

[5] Levy, L. L. Jr., "Experimental and Computational Steady and Unsteady Transonic Flows about a Thick Airfoil," *AIAA Journal*, Vol. 16, June 1978, pp. 564-572.

[6] Steger, J. L., "Implicit Finite-Difference Simulation of Flow about Arbitrary Two-Dimensional Geometries," *AIAA Journal*, Vol. 16, July 1978, pp. 679-686.

[7] Steger, J. L. and Bailey, H. E., "Calculation of Transonic Aileron Buzz," AIAA Paper 79-0134, Jan. 1979.

[8] Baldwin, B. S. and Lomax, H., "Thin Layer Approximation and Algebraic Model for Separated Turbulent Flows," AIAA Paper 78-257, Jan. 1978.

[9] Seegmiller, H. L., Marvin, J. G., and Levy, L. L. Jr., "Steady and Unsteady Transonic Flow," *AIAA Journal*, Vol. 16, Dec. 1978, pp. 1262-1270.

[10] Gault, D.E., "An Experimental Investigation of Regions of Separated Laminar Flow," NACA TN 3505, Sept. 1955.

AIAA 81-4300

Wind Tunnel Tests on Airfoils in Tandem Cascade

S. Raghunathan,* C. P. Tan,† and N.A.J. Wells‡
Queen's University of Belfast, Belfast, Northern Ireland

Nomenclature

C_T = tangential force coefficient, $F_t / \frac{1}{2}\rho w^2 cd$ (Fig. 1)
C_x = axial force coefficient, $F_x / \frac{1}{2}\rho w^2 cd$ (Fig. 1)
c = blade chord, m
d = blade span, m
l = distance between blades
Re = Reynolds number, WC/ν
S = solidity, c/l
W = freestream velocity, m/s
ρ = density of air, kg/m^3
ν = kinematic viscosity

Introduction

THE Wells turbine[1] is a self-rectifying axial flow turbine suitable for the extraction of energy from reversed cyclic airflows. These conditions are encountered in oscillating water column wave energy converters.

The Wells turbine rotor consists of several symmetric airfoil blades arranged around a central hub as shown in Fig. 1. The basic feature of the turbine is that even though the cyclic airflow produces oscillating axial forces on the airfoil blades, the tangential force on the rotor is always in the same direction.[2] This induces the rotation of the rotor and produces a power output without the need for sophisticated rectifying valves.

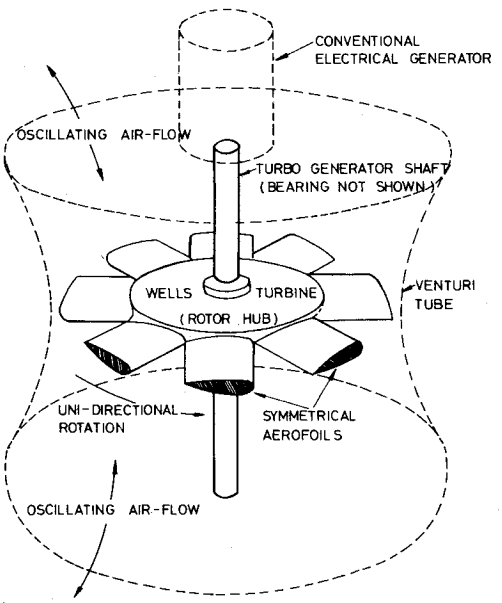

Fig. 1 Schematic of Wells turbine.

Received Dec. 29, 1980; revision received April 6, 1981.

*Lecturer, Dept. of Aeronautical Engineering.
†Research Student, Dept. of Aeronautical Engineering.
‡Part-time Research Student, Dept. of Civil Engineering.

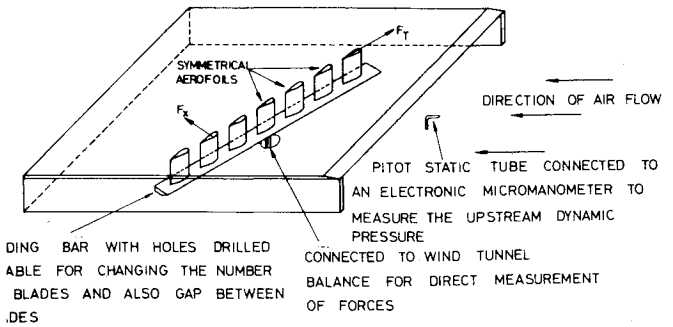

Fig. 2 Test setup.

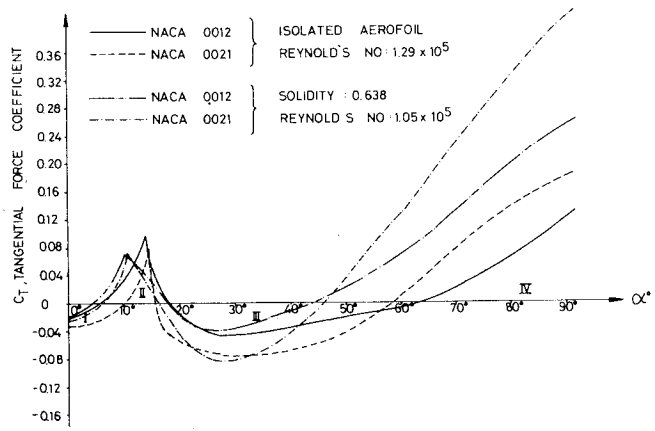

Fig. 3 Influence of thickness ratio on tangential force coefficient.

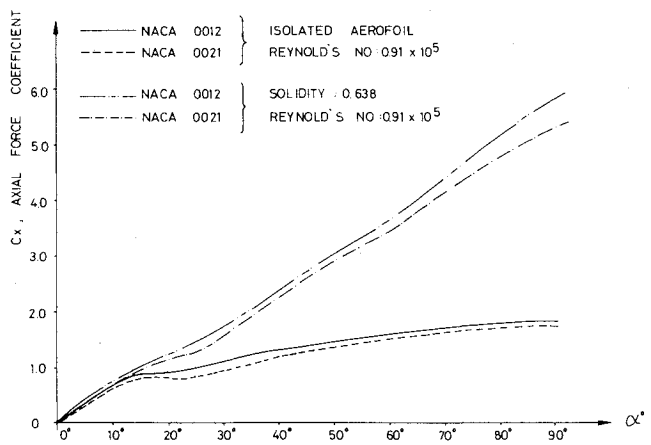

Fig. 4 Influence of thickness ratio on axial force coefficient.

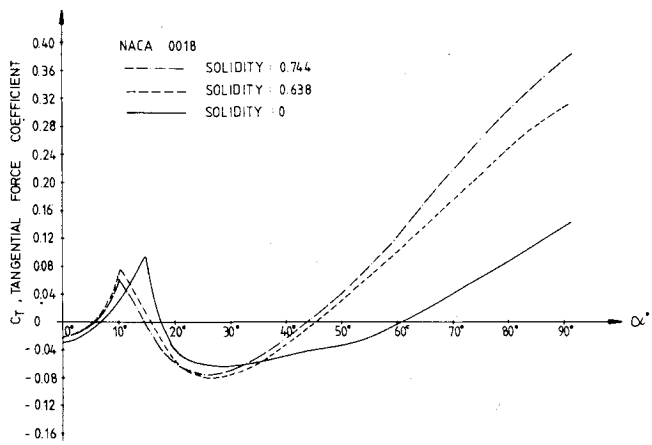

Fig. 5 Effect of solidity on tangential force coefficient.

Although considerable amounts of data are available on airfoil blades in a conventional cascade system (see, for example, Ref. 3), no experimental data are available for the case of airfoils in tandem cascade. This report describes some wind tunnel tests on NACA four-digit airfoils in a tandem cascade with the angles of incidence ranging from 0 to 90 deg.

Test Facility, Models, and Instrumentation

Tests were performed in a low-speed wind tunnel that had a maximum air velocity of 35 m/s. The airfoils used were the NACA 0012, 0018, and 0021. The airfoils had a chord of 85 mm and a span of 100 mm, and were located between a thin flat plate and a top plate as shown in Fig. 2. The clearance between the lower plate and the wind tunnel floor was 5 mm. The lower plate was fixed to a wind tunnel balance set on a turntable and located beneath the test section. This enabled the direct measurement of the tangential and normal forces on the blades. The freestream dynamic pressure was measured upstream of the cascade by a pitot tube. Tests were performed for several values of cascade solidities and at angles of incidence ranging from 0 to 90 deg. Reynolds number based on the blade chord was typically 10^5 and was limited by the length of the wind tunnel test section.

Results and Discussion

Figure 3 shows the variation of C_T with α for isolated blades (solidity 0) and for blades at solidity 0.638. Results here are shown for two thickness ratios and at a Reynolds number of 1.3×10^5. It is observed that C_T vs α curves consist of four regimes: regime 1, where C_T is negative and the negative values decrease with the increase in α; regime 2, where C_T values are positive initially increasing and then decreasing with α; regime 3, where C_T values are negative; and regime 4, where C_T values are positive and increase with α. In the case of the Wells turbine, the operating conditions will be in regime 2. It is observed that for the solidity of 0, the range of this regime decreases with the increase in the thickness ratio. The peak value of C_T also decreases with the increase in the thickness ratio. The incidence angle at which the stalling occurs, however, is postponed by the increase in the thickness. $\alpha = 90$ deg corresponds to the starting condition for the Wells turbine and the increase in thickness value has a favorable effect on starting. If the turbine has to move from the starting conditions to the operating regime, the turbine blades have to go through negative values of C_T in regime 3. The increase in the blade thickness results in larger negative values of C_T. Therefore, the advantage of a larger starting torque with a thicker profile is likely to be lost in its lesser tendency to accelerate toward the operating regime. The influence of thickness ratio on airfoils in cascade is similar to that observed for isolated airfoils, except that the peak value of C_T in regime 2 is rather insensitive to the thickness ratio.

The influence of α on C_X for the airfoils is seen in Fig. 4. For the isolated airfoils, the axial force increases with the increase in the angle of incidence. The value of C_X when starting is nearly twice that at the operating conditions. The flow separation at $\alpha = 90$ deg extends from the trailing edge to a point near the leading edge. The increase in the thickness ratio moves the point of separation downstream, which results in a decrease in C_X. The influence of thickness ratio on airfoils in cascade is similar to that deduced for isolated airfoils. However, a higher solidity has considerably increased the magnitude of C_X. End wall effects at low aspect ratio blades tested here enhance this further.

The effect of solidity on airfoils in cascade is shown in Fig. 5. Results here are shown for thickness ratios of 0.18 and solidities 0, 0.64, and 0.75. The airfoils in cascade have a lower peak value of C_T in regime 2 and stalls earlier when compared to an isolated airfoil. There were small differences in *Re* for the cases shown here.

An airfoil blade in tandem cascade has a higher peak negative value of C_T in regime 3, but has a smaller range for the negative values. There is a significant increase in both the values of C_T at $\alpha = 90$ deg and the range of regime 4. This suggests that the blades in cascades have better starting characteristics than an isolated blade, but will have a lower ultimate efficiency at the operating condition.

The study of self-starting characteristics is of critical importance in determining the characteristics of a rotor subjected to sinusoidal or random oscillatory flow, where the flow may cover a range of incidences in excess of stalling angle.

Finally, some comments about testing a finite number of airfoils in a tandem cascade. It has been observed that there is no significant changes in the values of C_T and C_X for 0 deg $< \alpha <$ 20 deg, provided a minimum number of blades (say 5-7) were used for a given solidity. However, changes in the value of C_X near $\alpha = 90$ deg were observed when the number of blades in the cascade were changed, with the resulting change in end conditions. The general trend was an increase in the value of C_X with the increase in the number of blades near $\alpha = 90$ deg. Results shown here, therefore, may be a slight underestimation of C_X in regime 4.

Acknowledgment

The authors wish to thank the members of the Wave Energy Group, Queen's University of Belfast for their help.

References

[1] Wells, A. A., private communication, Queen's University, Belfast, 1976.

[2] Raghunathan, S., "Theory and Performance of Wells Turbine," Rept. WE/80/13R, Queen's University of Belfast, 1980.

[3] "Turbine Design and Application," NASA SP 290, Vol. 1, 1973.

AIAA 80-1446R

Unsteady Wake of a Plunging Airfoil

Chih-Ming Ho* and Shin-Hsing Chen†
University of Southern California, Los Angeles, Calif.

Introduction

In many engineering applications (e.g., helicopters, turbines, compressors), lifting surfaces experience unsteady motion or are perturbed by unsteady incoming flows. High level dynamic loading and noise generation are inherent problems, due to unsteadiness.[1] For example, the blades in each stage of a multistage turbine or compressor are always under the unsteady loading imposed by the unsteady wake from previous stages. This problem[2,3] is commonly referred to as "wake cutting." However, the experimental results of unsteady wakes are very limited.[4] In the present study, the multiple hot-wire probe measurements and the on-line data acquisition system have significantly facilitated the study of an unsteady wake. Several interesting features of the wake of a plunging airfoil are presented in this Note.

Presented as Paper 80-1446 at the AIAA 13th Fluid and Plasma Dynamics Conference, July 14-16, 1980; submitted Sept. 24, 1980; revision received April 17, 1981.

*Associate Professor, Dept. of Aerospace Engineering. Member AIAA.

†Research Assistant, Dept. of Aerospace Engineering. Student Member AIAA.

Experimental Setup

The experiments were conducted in a low turbulence ($u'/U_0 < 0.02\%$) wind tunnel. The flow speed of the tunnel was varied from $U_0 = 2.5$ to 40 m/s. The airfoil used in the experiment has a NACA 0012 profile. The airfoil was molded from a high strength aluminum filled epoxy (DEVCON F2). The chord of the airfoil is $c = 10$ cm and the span is 53 cm. A pair of end plates was added on the airfoil in order to achieve two-dimensionality of the flow.

The driving mechanism of the plunging airfoil has a simple and versatile design, consisting of a dc motor, gears, eccentric wheels, and two shafts. The motor and gear combination can provide a wide variation of oscillation frequencies f. The maximum frequency is 20 Hz. The oscillation amplitude, determined by the eccentricity, is 0.32 cm. A phase referencing device is attached to the mechanism. An assembly consisting of a light source and a photo-transistor detects the passage of the driving gear and provides the triggering signal necessary in data reduction.

A miniature hot-wire rake was made to survey the flow. There are 10 hot-wires (five X-wires) on the rake. Each X-wire comprises two wires in X-array. The streamwise and transverse velocities could be measured by an appropriate combination of the angular sensitivities of the two cross wires. The cross section of each X-wire is 1.0×1.4 mm. The hot-wire rake is mounted on a traverse mechanism with three degrees-of-freedom. The movement in each direction is driven by a stepping motor that is controlled by a computer. All 10 hot-wire outputs were directly connected to the analog-digital converter interfaced to a PDP 11/55 minicomputer. The triggering signal was digitized with the hot-wire outputs and provided a phase reference for conditional sampling and ensemble averaging.

Experimental Results

In the investigation of the near wake of the plunging airfoil, 10 test cases covering a wide range of operating parameters were performed. The Reynolds number, $Re = U_0 c/\nu$, was varied from 2.1×10^4 to 10^5. The reduced frequency, $k = \omega c/2U_0$, was varied from 0 (stationary airfoil) to 1. Here ω is the angular frequency, $\omega = 2\pi f$. The angle of attack, θ, is 5 deg in all tests.

The instantaneous streamwise and transverse velocity components, u and v, are displayed in Fig. 1. A triggering pulse train is provided by a phase reference device on the driving mechanism. The triggering pulse in Fig. 1 indicates the time when the airfoil is at the lowest position during the oscillation. Features in the unsteady wake can be "visualized" simultaneously at several points across the entire wake. There are distinctly different characteristics in the upper and lower portions of the wake. The hot-wires located in the lower portion of the wake are intermittent inside and outside the

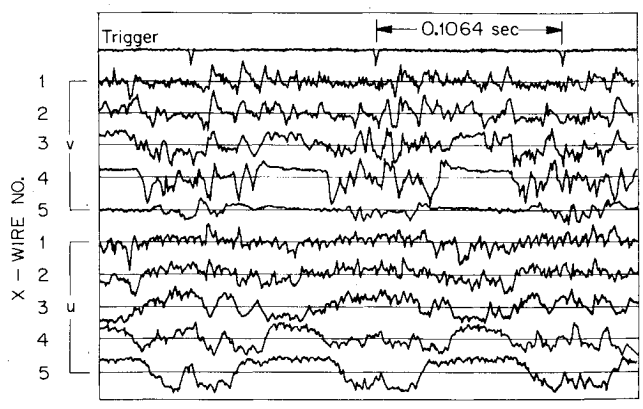

Fig. 1 Time record of velocity traces.